

# Complete Ion Spectra From a Simple Model of Nonlinear Shock Acceleration

Donald C. Ellison<sup>1</sup> and E.G. Berezhko<sup>2</sup>

<sup>1</sup>*Physics Department, North Carolina State University, Raleigh, NC 27695-8202, USA*

<sup>2</sup>*Institute of Cosmophysical Research and Aeronomy, Lenin Avenue 31, 677891 Yakutsk, Russia*

## Abstract

We describe a simple model of nonlinear diffusive shock acceleration which uses a three-power-law form for the accelerated particle spectrum, combined with a thermal distribution for the shock heated gas. The model contains the essential elements of the full nonlinear model and reliably reproduces exact numerical results with two arbitrary parameters: the injection rate and the maximum cutoff energy. We allow for either adiabatic or Alfvén wave heating of the upstream precursor and show how nonlinear effects influence the overall dynamics of the shock as well as the heating of the postshock gas.

## 1 Introduction:

Detailed studies using kinetic models (e.g., Berezhko et al. 1996; Berezhko & Völk 1997) clearly show that the shock *geometry* is the dominant factor which determines the maximum energy of particles in nonlinear shock acceleration. In the case of an expanding spherical shock, the acceleration process becomes unable, at some energy, to fill the upstream volume with high energy particles at the same number density as in the case of a plane shock of the same speed (Berezhko 1996). As a consequence, the cosmic ray (CR) spectrum cuts off near this energy. The cutoff energy is smaller than the maximum energy achieved in the same time in a plane shock. A different model, i.e., a steady-state, plane-shock approximation, also assumes that the shock geometry is the main factor that determines the shock structure (e.g., Jones & Ellison 1991). This is accomplished by including a free parameter,  $p_{\max}$ , which sets the maximum momentum particles can obtain (e.g., Ellison & Eichler 1984; Berezhko et al. 1987). This parameter, determined by geometrical factors, allows for a self-consistent, steady-state solution. The simple model described here is of this type and we claim that the specific mode of escape is unimportant and that models of evolving shocks and steady-state ones will produce essentially the same results for many parameter regimes (Berezhko & Ellison 1999). Thus, an evolving spherical shock can be approximated by a sequence of quasi-stationary states making the plane-shock, steady-state approximation we describe here useful.

A complete description of our simple model is given in Berezhko & Ellison (1999). Briefly, we have developed a set of algebraic equations (easy to describe and solve) which includes the essential nonlinear effects of efficient acceleration. By direct comparison with exact solutions, we have shown that the simple model not only gives a qualitative description of nonlinear shock acceleration, but also provides quite good *quantitative* results sufficient for many astrophysical applications.

## 2 Model:

For superthermal particles, we approximate  $f(p)$ , the momentum phase space distribution, with

$$f(p) = \begin{cases} a_{\text{inj}}(p/p_{\text{inj}})^{-q_{\text{sub}}} & \text{if } p_{\text{inj}} \leq p \leq mc , \\ a_{\text{mc}}[p/(mc)]^{-q_{\text{int}}} & \text{if } mc \leq p \leq p_{\text{int}} , \\ a_{\text{max}}(p/p_{\text{int}})^{-q_{\text{min}}} & \text{if } p_{\text{int}} \leq p \leq p_{\text{max}} . \end{cases} \quad (1)$$

The spectral indexes are:  $q_{\text{sub}} = 3r_{\text{sub}}/(r_{\text{sub}} - 1)$ ,  $q_{\text{min}} = 3.5 + (3.5 - 0.5 r_{\text{sub}})/(2 r_{\text{tot}} - r_{\text{sub}} - 1)$  (from Berezhko 1996), and  $q_{\text{int}} = (q_{\text{tp}} + q_{\text{min}})/2$ , where  $r_{\text{sub}}$  is the subshock compression ratio,  $r_{\text{tot}}$  is the overall compression ratio, and  $q_{\text{tp}}$  is the test-particle index given by  $q_{\text{tp}} = 3r_{\text{tot}}/(r_{\text{tot}} - 1)$ . The normalizations are:

$a_{mc} = a_{inj} [p_{inj}/(mc)]^{q_{sub}}$ ,  $a_{max} = a_{mc} (mc/p_{int})^{q_{int}}$ , where  $a_{inj}$  is defined below,  $p_{inj}$  is the injection momentum, and  $p_{max}$  is the maximum (i.e., cutoff) momentum. Particles obtaining  $p_{max}$  escape from the system and carry away energy. In a plane-wave approach,  $p_{max}$  is a free parameter. The intermediate momentum,  $p_{int}$ , is chosen (by comparison with exact numerical solutions) to be  $p_{int} = \max(mc, 0.01p_{max})$ . We define  $p_{inj} = \lambda m (u_0/r_{tot}) \sqrt{\gamma_g(r_{sub} - 1)}$ , where  $u_0$  is the shock speed,  $m$  is the particle mass (only protons here),  $\lambda$  is a constant injection parameter taken to be 4.3 for consistency with previous work, and  $\gamma_g = 5/3$  is the ratio of specific heats for the thermal gas. Particles with  $p < mc$  are taken to be fully nonrelativistic and those with  $p > mc$  to be fully relativistic. One more injection parameter,  $\eta$ , determines the number of gas particles injected:  $N_{inj} = \eta N_{g1}$ , where  $N_{g1} = \rho_1/m$  is the gas number density just upstream from the subshock. The injection rate,  $\eta = N_{inj}/N_{g1}$ , sets the overall efficiency of the acceleration. From particle conservation, we find  $a_{inj} = N_{inj} q_{sub}/(4\pi p_{inj}^3)$ . Everywhere, the subscript ‘0’ implies far upstream, ‘1’ indicates values just upstream of the subshock, and ‘2’ implies downstream.

The accelerated particle pressure is  $P_{en} = (4\pi/3) \int_{p_{inj}}^{p_{max}} dp p^3 v f(p)$  and the simple form for the distribution function given in (1) makes it possible to calculate the total pressure of energetic particles  $P_{en} = P_{nr} + P_{rel}$  as the sum of pressures from non-relativistic  $P_{nr}$  and relativistic particles  $P_{rel} = P_{rel,low} + P_{rel,high}$ , i.e.,

$$P_{nr} = \begin{cases} \frac{\eta r_{tot}}{(r_{sub}-1)^{(5-q_{sub})}} \left(\frac{p_{inj}}{mc}\right)^{q_{sub}-3} \left[1 - \left(\frac{p_{inj}}{mc}\right)^{5-q_{sub}}\right] \rho_0 c^2 & \text{if } q_{sub} \neq 5, \\ \frac{\eta r_{tot}}{r_{sub}-1} \left(\frac{p_{inj}}{mc}\right)^2 \ln\left(\frac{mc}{p_{inj}}\right) \rho_0 c^2 & \text{if } q_{sub} = 5, \end{cases} \quad (2)$$

$$P_{rel,low} = \begin{cases} \frac{\eta r_{tot}}{(r_{sub}-1)^{(4-q_{int})}} \left(\frac{p_{inj}}{mc}\right)^{q_{sub}-3} \left[\left(\frac{p_{int}}{mc}\right)^{4-q_{int}} - 1\right] \rho_0 c^2 & \text{if } q_{int} \neq 4, \\ \frac{\eta r_{tot}}{r_{sub}-1} \left(\frac{p_{inj}}{mc}\right)^{q_{sub}-3} \ln\left(\frac{p_{int}}{mc}\right) \rho_0 c^2 & \text{if } q_{int} = 4, \end{cases} \quad (3)$$

and

$$P_{rel,high} = \begin{cases} \frac{\eta r_{tot}}{(r_{sub}-1)^{(4-q_{min})}} \left(\frac{p_{inj}}{mc}\right)^{q_{sub}-3} \left(\frac{p_{int}}{mc}\right)^{4-q_{int}} \left[\left(\frac{p_{max}}{p_{int}}\right)^{4-q_{min}} - 1\right] \rho_0 c^2 & \text{if } q_{min} \neq 4, \\ \frac{\eta r_{tot}}{r_{sub}-1} \left(\frac{p_{inj}}{mc}\right)^{q_{sub}-3} \left(\frac{p_{int}}{mc}\right)^{4-q_{int}} \ln\left(\frac{p_{max}}{p_{int}}\right) \rho_0 c^2 & \text{if } q_{min} = 4. \end{cases} \quad (4)$$

For typical SNR parameters,  $p_{inj} \ll mc$ ,  $q_{sub} > 4$ , and  $p_{max} \gg mc$ , providing  $P_{rel} \gg P_{nr}$ .

Since the subshock is an ordinary gas shock, its compression ratio is determined by the subshock Mach number,  $M_{S1}$ , i.e.,  $r_{sub} = [(\gamma_g + 1) M_{S1}^2] / [(\gamma_g - 1) M_{S1}^2 + 2]$ . The subshock Mach number in turn can be related to the far upstream sonic Mach number,  $M_{S0}$ , by  $M_{S1} = M_{S0} (\rho_0/\rho_1)^{(\gamma_g+1)/2} = M_{S0} (r_{sub}/r_{tot})^{(\gamma_g+1)/2}$  if the gas is heated *adiabatically* in the precursor region, i.e.,  $P_g \propto \rho^{\gamma_g}$ , and conservation of mass flux,  $\rho_1 u_1 = \rho_0 u_0$ , through the subshock transition is used. With momentum and energy conservation, we can write,

$$u_1/u_0 = r_{sub}/r_{tot} = 1 - P_{en}/(\rho_0 u_0^2) - (P_{g1} - P_{g0})/(\rho_0 u_0^2), \quad (5)$$

where  $P_{g1} = P_{g0} (r_{tot}/r_{sub})^{\gamma_g}$  is the gas pressure just upstream from the subshock and  $P_{g0} = \rho_0 u_0^2 / (\gamma_g M_{S0}^2)$  is the far upstream gas pressure.

The above set of equations can be solved to provide all the shock parameters including:  $r_{tot}$ ,  $r_{sub}$ , the escaping energy, and the overall acceleration efficiency as a function of  $M_{S0}$ ,  $\eta$ , and  $p_{max}$ . These, in turn, give the spectral indexes needed in (1) to find the spectrum above  $p_{inj}$ . We approximate the thermal component with a Maxwell-Boltzmann distribution at the downstream density and gas pressure and smoothly add this to the energetic distribution. The downstream gas pressure is  $P_2 \approx (u_0/r_{tot})^2 (r_{sub} - 1)$ , and  $n_2 = r_{tot} n_0$ .

For high Mach numbers, additional gas heating can change the results dramatically and lower the overall compression ratio. We consider Alfvén wave dissipation as described by Völk, Drury, & McKenzie (1984):

$$u \frac{\partial}{\partial x} (P_g \rho^{-\gamma_g}) = (\gamma_g - 1) c_A \frac{\partial P_{en}}{\partial x} \rho^{-\gamma_g}, \quad (6)$$

where  $c_A = B/\sqrt{4\pi\rho}$  is the Alfvén speed ( $M_{A0} = u_0/c_{A0}$  is the far upstream Alfvén Mach number) and we assume a constant Alfvén speed  $c_A = c_{A0}$ . Approximately,

$$P_{g1}/P_{g0} \simeq (\rho_1/\rho_0)^{\gamma_g} \{1 + (\gamma_g - 1)(M_{S0}^2/M_{A0})[1 - (\rho_0/\rho_1)^{\gamma_g}]\}. \quad (7)$$

### 3 Results:

Fig. 1. shows a comparison between the simple model (dashed line) and an exact Monte Carlo calculation (solid line) with the same parameters. The self-consistent Monte Carlo result conserves mass, momentum, and energy fluxes; the energy flux carried by particles escaping at  $p_{\max}$  is included in determining the shock dynamics; the ratio of specific heats of the shocked gas is determined with the proper weighting of nonrelativistic, trans-relativistic, and fully relativistic particles; and there is no distinction between thermal and superthermal particles, i.e., the injection of particles occurs directly from the shocked heated gas. We plot  $p^4 f(p)$  (in dimensionless units) to flatten the spectra and make the distinctive upward curvature more obvious.

The injection efficiency for the dashed line,  $\eta = 5 \times 10^{-3}$ , gives efficient acceleration and a highly nonlinear result. Here,  $r_{\text{tot}} \sim 50$  giving a flat spectrum at high momenta with the large majority of particle pressure in the high energy end of the distribution. The structure of the shock is such, however, that the subshock is quite weak ( $r_{\text{sub}} = 2.68$ ) resulting in a relatively low shocked temperature. If the injection efficiency is considerably lower, as in the  $\eta = 5 \times 10^{-5}$  example (dot-dashed line), an essentially test-particle solution results with  $r_{\text{sub}} \sim r_{\text{tot}} \sim 4$ . Note the large difference in the downstream temperatures between the nonlinear and test-particle results. As stated above,  $\eta$  is an arbitrary parameter in the simple model and some indications from observations and from plasma simulations suggest that injection rates in actual shocks are close to the value obtained in the Monte Carlo simulations (e.g., Ellison, Möbius, & Paschmann 1990; Giacalone et al. 1993). An important aspect of Fig. 1 is the fact that even though  $r_{\text{tot}}$  is extremely large (for the Monte Carlo result and for  $\eta = 5 \times 10^{-3}$  for the simple model), the spectral index near  $p_{\max}$  is close to  $q_{\min} = 3.5$  rather than  $\sim 3$  predicted by test-particle theory. The expression we use for  $q_{\min}$  was derived by perturbation methods which are only strictly valid for slightly modified shocks, however, there are quantitative arguments which prove that our expression is a close approximation for strongly modified shocks as well (Berezhko 1996). At high compression ratios,  $r_{\text{tot}} \gg r_{\text{sub}}$  and the spectral index approaches  $q_{\min} \rightarrow 3.5$  instead of 3. This limit agrees with the analysis performed for strongly modified shocks by Malkov (1997).

In Fig. 2 we show  $r_{\text{tot}}$  and  $r_{\text{sub}}$  from the simple model as a function of  $M_{S0}$  for three  $\eta$ 's and with a constant unshocked temperature,  $T_0 = 10^6$  K. These results could represent an evolving SNR shock as it slows and weakens. The shock speed and  $M_{A0}$  vary with  $M_{S0}$ , and the two panels have different values of unshocked magnetic field and density. For large  $\eta$ ,  $r_{\text{tot}}$  increases monotonically with  $M_{S0}$  or since  $M_{S0} \approx 18M_{A0}$  in the top panel,  $r_{\text{tot}} \approx 1.5M_{A0}^{3/8}$  ( $M_{S0} \approx M_{A0}$  in the lower panel). The dotted line is for  $\eta = 10^{-2}$  with only adiabatic heating and here,  $r_{\text{tot}} \approx 1.3M_{S0}^{3/4}$ . At high  $M_{S0}$ , and with strong injection, the shocks are very efficient placing  $\gtrsim 50\%$  of the far upstream energy flux into relativistic particles, a large fraction of which

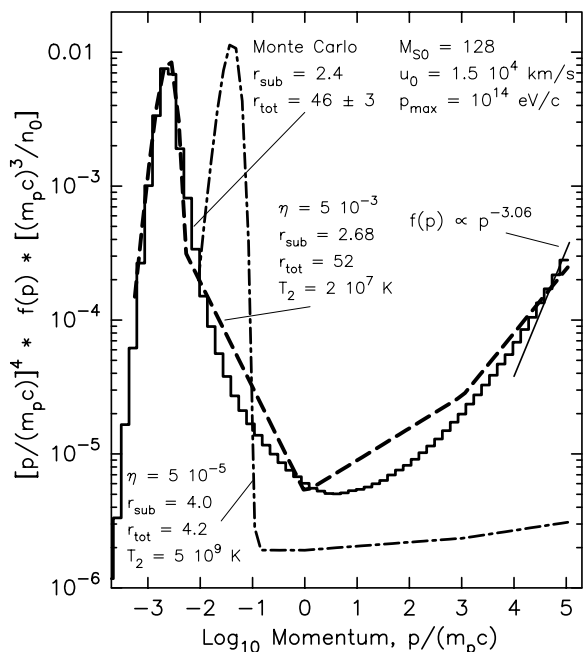


**Figure 1:** The  $\eta = 5 \times 10^{-3}$  case is chosen to match the Monte Carlo result, and the Monte Carlo spectrum is plotted in the downstream plasma frame. The model spectra are considerably steeper than the test-particle prediction,  $f \propto p^{-3.06}$  (solid line), at the highest momenta.

can be in escaping particles. If  $\eta$  is low enough however, strong, *unmodified* shocks can result. The dot-dashed lines in Fig. 2. ( $\eta = 10^{-4}$ ) show the relatively abrupt transition from the strongly modified state to the unmodified state as  $M_{S0}$  increases.

## 4 Conclusions:

We present a simple model of nonlinear shock acceleration which is easy to calculate, contains the essential features of the acceleration process and nonlinear shock structure, and corresponds closely with exact Monte Carlo simulations and kinetic results. The model is based on a three-power-law approximation of the energetic particle distribution plus a thermal peak at the downstream temperature and density, producing a full spectrum (see Berezhko & Ellison 1999 for more details).

While this model is for plane-parallel, steady-state shocks, we claim these approximations are not highly restrictive and that the model can be extended to describe evolving systems such as supernova remnants (Ellison & Berezhko 1999). The model shows that as  $M_{S0}$  increases, the shock becomes more modified, i.e.,  $r_{tot} \simeq 1.3 M_{S0}^{3/4}$ , and energetic particles absorb almost all of the shock energy if the shock speed  $u_0$  is lower than some critical value,  $u_0^* \sim 5\eta\lambda[p_{max}/(mc)]^{1/4}c$  (see Berezhko & Ellison 1999). For  $u_0 < u_0^*$ , acceleration is efficient and the shock is strongly modified by the backpressure of the energetic particles. If  $u_0 > u_0^*$ , the shock, although still strong, becomes almost unmodified and accelerated particle production decreases inversely proportional to  $u_0$ . The increase in  $r_{tot}$  above 4 results mainly from the escaping energy flux. For some parameters, as much as 90% of the energy flux is placed in escaping particles. Such large escaping fluxes should play an extremely important role in the dynamics of real expanding shocks.

**Acknowledgments:** EGB acknowledges the hospitality of North Carolina State University where the main part of this work was carried out. This work was supported in part by the Russian Foundation for Basic Research (97-02-16132) and NASA's Space Physics Theory Program.

Berezhko, E.G. 1996, *Astroparticle Phys.*, **5**, 367

Berezhko, E.G., & Ellison, D.C. 1999 *Ap. J.*, submitted

Berezhko E.G., Yelshin, V.K., Krymsky, G.F. & Turpanov, A.A. 1987, in *Proc. 20th ICRC(Moscow)*, **2**, 175

Berezhko, E.G., Yelshin, V.K. & Ksenofontov, L.T. 1996, *ZhETF*, **109**, 3.

Berezhko, E.G. & Völk, H.J. 1997, *Astroparticle Phys.*, **7**, 183

Ellison, D.C., & Berezhko, E.G. 1999, *Ap.J.*, in preparation

Ellison, D.C., & Eichler, D., 1984, *Ap.J.*, **286**, 691

Ellison, D.C., Möbius, E., & Paschmann, G. 1990, *Ap.J.*, **352**, 376

Giacalone, J., Burgess, D., Schwartz, S.J. & Ellison, D.C. 1993, *Ap.J.*, **402**, 550

Jones, F.C., & Ellison, D.C. 1991, *Space Sci. Rev.*, **58**, 259

Malkov, M. 1997, *Ap.J.*, **485**, 638

Völk, H.J., Drury, L.O'C., & McKenzie, J.F. 1984, *A&A*, **130**, 19

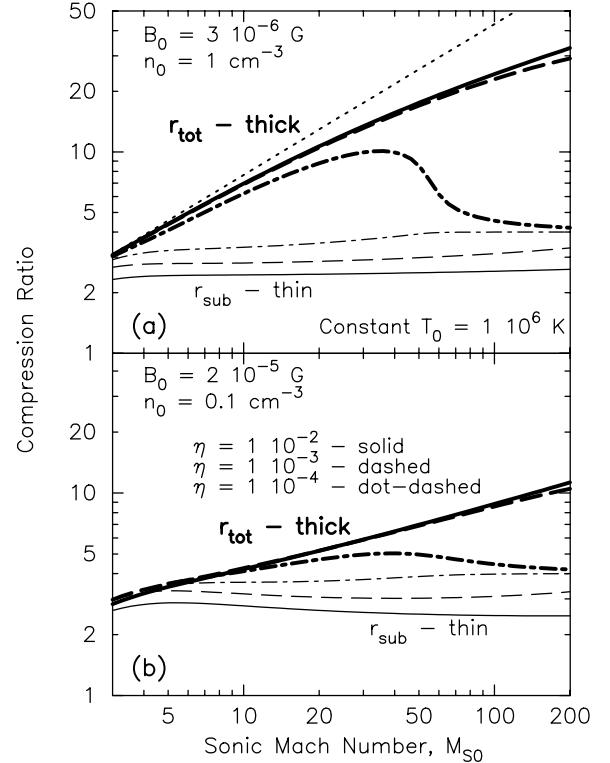


**Figure 2:**  $r_{tot}$  and  $r_{sub}$  vs.  $M_{S0}$ . In both panels, the upstream temperature is kept constant as  $u_0$  and  $M_{S0}$  varies. The dotted line in the top panel is  $r_{tot}$  for  $\eta = 10^{-2}$  with only adiabatic heating. All other curves include Alfvén wave heating as described in eqn. (7)